AD-A127 118 THEORETICAL INVESTIGATION OF THREE-DIMENSIONAL SHOCK WAVE-TURBULENT BOUND..(U) RUTGERS - THE STATE UNIV NEW BRUNSWICK N J DEPT OF MECHANICAL.. D D KNIGHT DEC 82 1/1

UNCLASSIFIED RU-TR-157-MAE-F AFOSR-TR-83-0230 F/G 20/4 NL

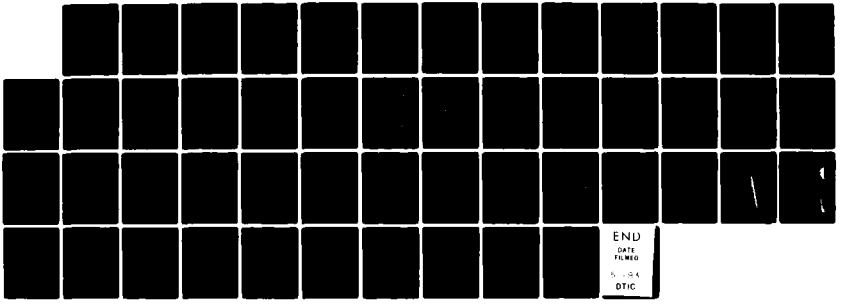

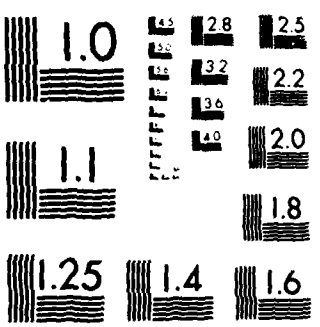

AFOSR-TR- 83-0230

Report RU-TR-157-MAE-F

THEORETICAL INVESTIGATION OF THREE-DIMENSIONAL SHOCK WAVE-TURBULENT BOUNDARY LAYER INTERACTIONS

Doyle D. Knight
Department of Mechanical and Aerospace Engineering
Rutgers University
New Brunswick, New Jersey 08903

December 1982

Interim Report for Period 1 October 1981 to 30 September 1982

Approved for Public Release - Distribution Unlimited

Air Force Office of Scientific Research
Building 410
Bolling AFB
Washington, DC 20332

UNCLASSIFIED

SECURITY CLASSIFICATION OF THIS PAGE (When Data Entered)

REPORT DOCUMENTATION PAGE	READ INSTRUCTIONS BEFORE COMPLETING FORM
1. REPORT NUMBER: AFOSR-TR- 83-0230	2. GOVT ACCESSION NO.: AD A127118
3. RECIPIENT'S CATALOG NUMBER	
4. TITLE (and Subtitle): THEORETICAL INVESTIGATION OF THREE-DIMENSIONAL SHOCK WAVE-TURBULENT BOUNDARY LAYER INTERACTIONS	5. TYPE OF REPORT & PERIOD COVERED: Interim - Annual, 1 Oct 1981 - 30 Sept 1982
	6. PERFORMING ORG. REPORT NUMBER
7. AUTHOR(s): Prof. Doyle D. Knight	8. CONTRACT OR GRANT NUMBER(s): AFOSR-82-0040
9. PERFORMING ORGANIZATION NAME AND ADDRESS: Dept. of Mechanical and Aerospace Engineering, Rutgers University, New Brunswick, New Jersey 08903	10. PROGRAM ELEMENT, PROJECT, TASK AREA & WORK UNIT NUMBERS: 61102F, 2307/K1
11. CONTROLLING OFFICE NAME AND ADDRESS: Air Force Office of Scientific Research/NM, Building 410, Bolling AFB, Washington, DC 20332	12. REPORT DATE: December 1982
	13. NUMBER OF PAGES: 44
14. MONITORING AGENCY NAME & ADDRESS(if different from Controlling Office)	15. SECURITY CLASS. (of this report): UNCLASSIFIED
	15a. DECLASSIFICATION/DOWNGRADING SCHEDULE

16. DISTRIBUTION STATEMENT (of this Report)

Approved for Public Release; Distribution Unlimited.

17. DISTRIBUTION STATEMENT (of the abstract entered in Block 20, if different from Report)

18. SUPPLEMENTARY NOTES

19. KEY WORDS (Continue on reverse side if necessary and identify by block number)

High Speed Flows; Viscous-Inviscid Interactions; Shock-Boundary Layer Interactions; Computational Fluid Dynamics; Navier-Stokes Equations; Turbulence

20. ABSTRACT (Continue on reverse side if necessary and identify by block number)

The overall focus of the research effort is the understanding of the physical structure of 3-D shock wave-turbulent boundary layer interactions. The approach utilizes the full mean compressible Navier-Stokes equations with turbulence incorporated through the algebraic turbulent eddy viscosity model of Baldwin and Lomax. The research effort is categorized into two major areas. First, the efficacy of the Baldwin-Lomax model is examined

DD FORM 1 JAN 73 1473 EDITION OF 1 NOV 65 IS OBSOLETE

UNCLASSIFIED

SECURITY CLASSIFICATION OF THIS PAGE (When Data Entered)

cont'd for the 2-D supersonic compression ramp at Mach 3 and a Reynolds number based on upstream boundary layer thickness of 1.6 million. The flowfields corresponding to ramp angles of 8 deg to 24 deg have been computed, and two simple modifications to the Baldwin-Lomax model have been suggested and evaluated. The results indicate that the Baldwin-Lomax model underestimates the upstream propagation of the shock-boundary layer interaction, and underestimates the recovery of the boundary layer downstream of reattachment. The incorporation of a simple relaxation modification to the eddy viscosity greatly improves the prediction of the upstream propagation, but does not appreciably affect the prediction of the downstream recovery of the boundary layer. Second, the three-dimensional interaction of an oblique shock wave with a turbulent boundary layer (the 3-D "sharp fin" configuration) at Mach 3 has been computed for two different shock strengths (i.e., shock-generator angles), and the results compared with the extensive experimental data. Present results indicate that the Baldwin-Lomax model provides an accurate prediction of a wide variety of flow properties, including surface pressure, heat transfer, yaw and pitch angle, static pressure and pitot pressure.

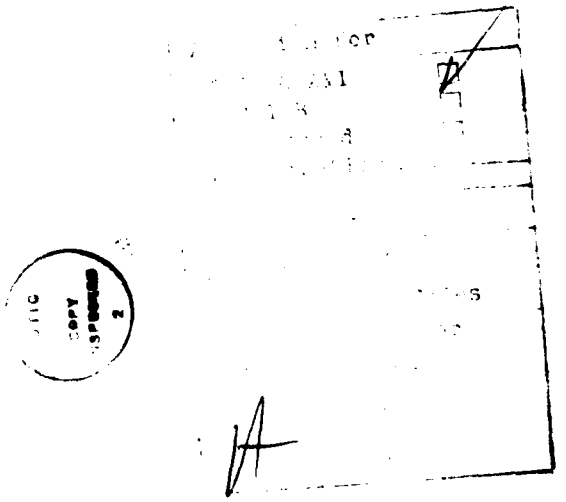

PREFACE

This report presents the research accomplishments for the period 1 October 1981 to 30 September 1982 for the research investigation entitled "Theoretical Investigation of Three-Dimensional Shock Wave-Turbulent Boundary Layer Interactions." The research has profited from the generous assistance of numerous individuals. The assistance of Dr. James Wilson, Air Force Office of Scientific Research, is gratefully acknowledged. The important and helpful interactions with Prof. Seymour Bogdonoff, Dr. Dave Dolling, Dr. Gary Settles and Prof. Lex Smits of Princeton University have contributed to the success of the research effort. The assistance of Dr. James Keller and Dr. Jerry South and the staff of the Analysis and Computation Division at NASA Langley Research Center is also gratefully noted.

TABLE OF CONTENTS

LIST OF ILLUSTRATIONS

I. Introduction

The phenomenon of three-dimensional shock wave-turbulent boundary layer interaction (denoted "D-D turbulent interactions for brevity) represents an important unsolved problem in modern high speed fluid mechanics. It is present in a wide variety of fluid flow applications, including high speed aerodynamics (e.g., the deflection of aerodynamic control surfaces), internal flows (e.g., high speed aircraft inlets) and gas dynamic lasers.[1] A complete physical understanding of 3-D turbulent interactions is lacking even for simple geometries,[2] and thus further research effort is warranted in this area.

The overall goals of the present research program, as indicted in the original proposal,[3] are the following:

1. To determine the accuracy of theoretical predictions of 3-D shock wave-turbulent boundary layer interactions by numerical solution of the three-dimensional mean compressible Navier-Stokes equations with a turbulent eddy viscosity model.

2. To investigate the physical structure of 3-D shock wave-turbulent boundary layer interactions in simplified geometries (e.g., swept compression corner, swept fin and sharp fin configurations) through a close cooperative research effort consisting of numerical computations by the present investigator and experimental studies by the Princeton Gas Dynamics Laboratory.

3. To evaluate the hypothesized physical structure of 3-D interactions at a variety of conditions outside the range of the experiments (e.g., different Mach numbers and geometries).

The research effort during the first year has focused on two major areas. First, the accuracy of the algebraic turbulent eddy viscosity model has been examined for 2-D turbulent interactions for the configuration of a 2-D supersonic compression corner at Mach 3. Second, the three-dimensional interaction of an oblique shock with a turbulent boundary layer for the 3-D sharp fin configuration has been evaluated. The results are presented in detail in the following sections.

II. Status of the Research for First Year

and

Schedule of Research for Remainder of Second Year

A. Calculation of Two-Dimensional Turbulent Compression Ramp Flows

1. Motivation

The purpose of the 2-D supersonic compression ramp investigation is to critically examine the efficacy of the algebraic turbulent eddy viscosity model, developed by Baldwin and Lomax,[4] for the computation of 2-D turbulent interactions. This turbulence model, which has also been adopted for the 3-D turbulent interaction investigation, has been employed for a variety of 3-D flowfield calculations.[3,5-8] The Baldwin-Lomax model, however, has not been critically examined for 2-D turbulent interactions. The major focus of this research is to identify the deficiencies of the Baldwin-Lomax model for this type of flows, and to develop sensible modifications, within the inherent limitations of the algebraic eddy viscosity concept, that would result in improvements to the overall flowfield prediction.

2. Experimental Configuration

The flow configuration is illustrated in Fig. 1. An equilibrium supersonic turbulent boundary layer is turned by the deflection of a ramp of variable angle α. An extensive experimental data base has been acquired by Settles and his colleagues at the Princeton Gas Dynamics Laboratory[9-11] at a nominal Mach number of 2.9. The data may be categorized into two major areas, namely (1) flowfield profiles for four corner angles at a fixed Reynolds number Re_{δ_∞} of 1.6 million, and (2) surface pressures for a fixed ramp angle of 20 deg for a range of Reynolds numbers Re_{δ_∞} from 0.75 million to 7.6 million. The

FLØW CØNFIGURATIØN

2-D CØMPRESSIØN RAMP

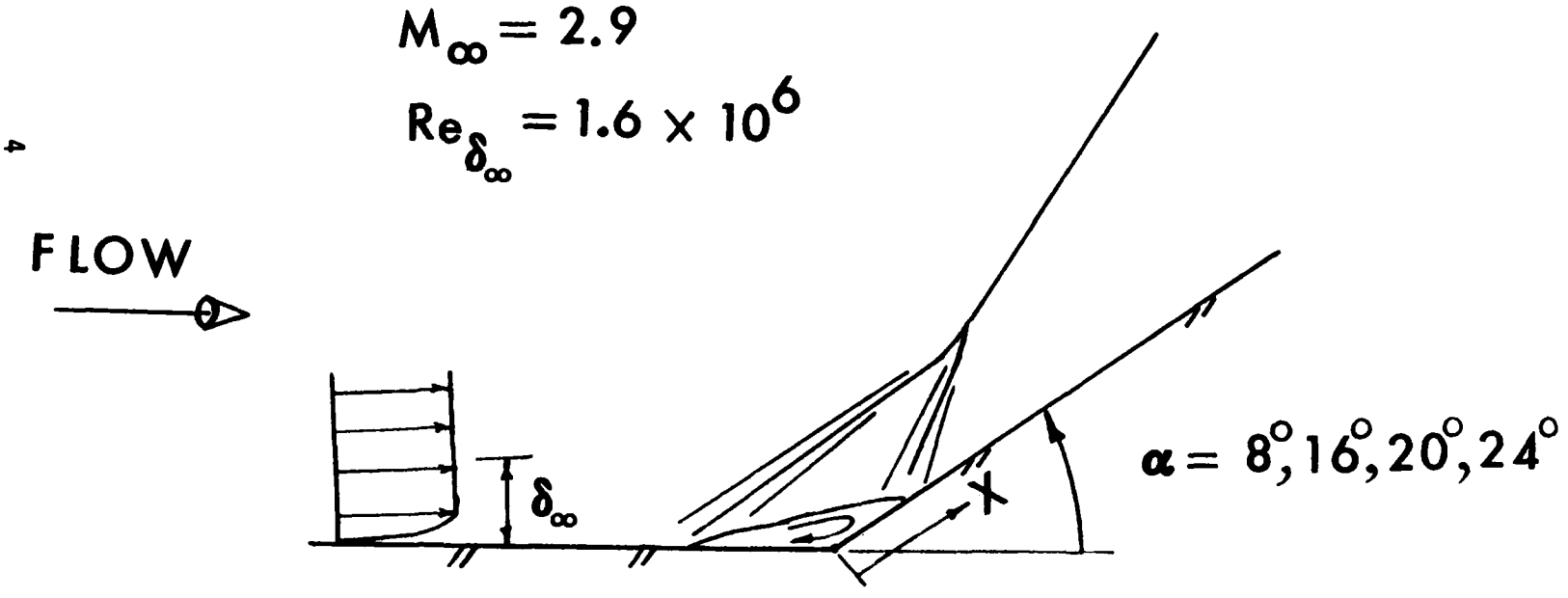

Fig. 1. Geometry of 2-D Supersonic Compression Ramp

first category includes measurements of (a) surface pressure, (b) skin friction, and (c) velocity, Mach number and static pressure profiles at nine streamwise stations for each ramp angle. The second category includes surface pressure and separation-to-reattachment length data.

3. Method of Solution

The governing equations are the full mean compressible Navier-Stokes equations in two dimensions using mass-averaged variables,[12] strong conservation form,[13] and general curvilinear coordinates. In addition, the equation of state for a perfect gas, and Sutherland's relation for the molecular viscosity are used. The molecular and turbulent Prandtl numbers are 0.72 (air) and 0.9, respectively.

The algebraic turbulent eddy viscosity model of Baldwin and Lomax is employed. Two additional modifications were made to the turbulence model during the course of the investigation. To date, therefore, three different versions have been employed as follows:

a. Unmodified Baldwin-Lomax Model

This is the original form proposed by Baldwin and Lomax.[4]

b. Modified Baldwin-Lomax Model

In this version, the local value of the shear stress is employed in the Van Driest damping factor. In addition, the outer form of the eddy viscosity is modified to reduce unphysical oscillations in the computed turbulent length scale in the vicinity of the compression corner.

c. Baldwin-Lomax Model with Relaxation

This version employs the relaxation eddy viscosity model proposed by Shang and Hankey[14] for the Cebeci-Smith turbulence model. The equilibrium eddy viscosity is the modified Baldwin-Lomax model.

The numerical algorithm employed to solve the Navier-Stokes equations is the implicit approximate factorization method of Beam and Warming.[15] The algorithm is second-order accurate, and is widely used for 2-D and 3-D flow-field calculations.

The incoming boundary layer profile, which provides the upstream boundary condition for the computations, was obtained by calculating the development of a flat plate turbulent boundary layer up to the station where the computed and experimental momentum thicknesses were equal. The computed upstream profile is in close agreement with the experiment[9-11] and the compressible Law of the Wall and Wake.[16]

A typical computational grid is highly non-uniform in both coordinate directions in order to provide sufficient resolution of the turbulent boundary layer and the interaction region. The normal mesh spacing near the wall was chosen to accurately resolve the viscous sublayer, with Δy^+ less than approximately two at all stations. The typical number of grid points within the boundary layer was 25 to 30 at all stations. The streamwise grid spacing in the interaction region varied from 0.027 δ_∞ (for α = 8 deg) to 0.077 δ_∞ (for α = 24 deg). The maximum streamwise grid spacing outside the corner interaction region was always less than 0.6 δ_∞ .

4. Results

During the first year, the research effort in the 2-D supersonic compression ramp focused on the first cagegory of the experimental data base, namely, the examination of the effects of ramp angle for a fixed Reynolds number Re_{δ_∞}. Research is continuing in this area during the second year, with the purpose of completing the computation of all four cases with the modified and relaxation versions of the Baldwin-Lomax model. For those cases presented in this report, a full comparison of the computed results with the experimental data has been

performed. For purposes of brevity, the results presented herein have been limited.

4.1 Results for 8 deg Ramp

The computed and measured surface pressure for the 8 deg ramp is displayed in Fig. 2. The ordinate is the surfacepressure, normalized by the upstream static pressure, and the abscissa is the distance from the corner normalized by the upstream boundary layer thickness δ_∞. The computed and measured profiles are seen to be in good agreement in the interaction region. Downstream of the interaction, the computed pressure is slightly above the experimental results, although the maximum deviation of approximately 3% is only slightly greater than the experimental uncertainty (2%) indicated in Ref. 11.

The computed and measured surface shear stress, normalized by the upstream dynamic pressure, is shown in Fig. 3. Upstream of the interaction, the computed and measured values are in close agreement, as indicated above. The computed and experimental profiles display an abrupt decrease associated with the shock-boundary layer interaction at the corner. The computed profile shows a small separated region approximately 1.4 mm in length. The experimental skin friction displays a positive minimum value. However, the distance between successive skin friction measurements in the corner region (2.5 mm) is nearly twice the size of the computed separation region, and hence the separation region is unlikely to be observed in the experiments. Although the kerosene-graphite visualization did not display any evidence of separation for the 8 deg ramp, it is possible that the scale of the separation is below the resolution of the kerosene-graphite technique.

4.2 Results for 16 deg Ramp

Two separate calculations were performed for the 16 deg ramp, using the

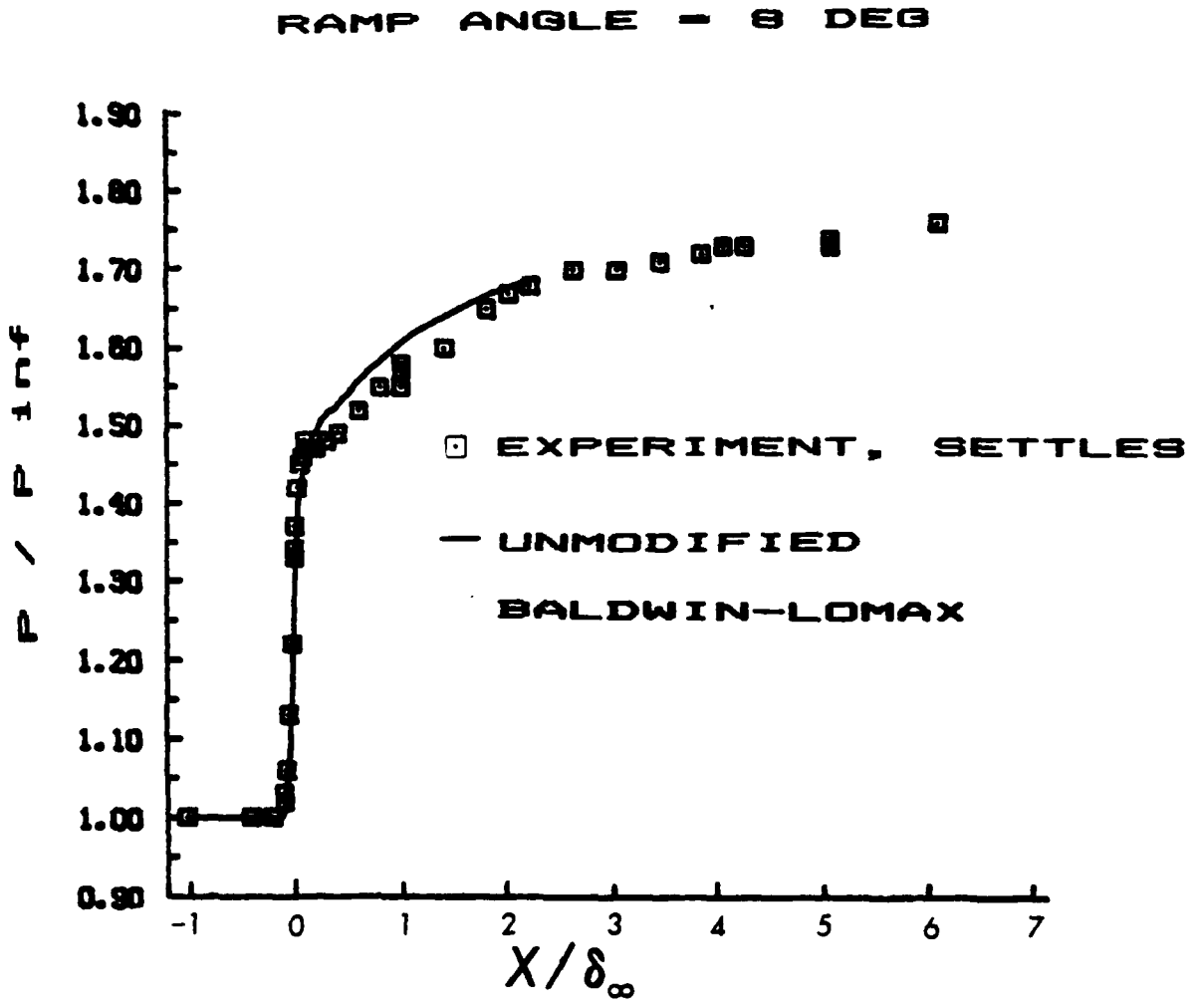

Fig. 2. Surface Pressure for α = 8 deg

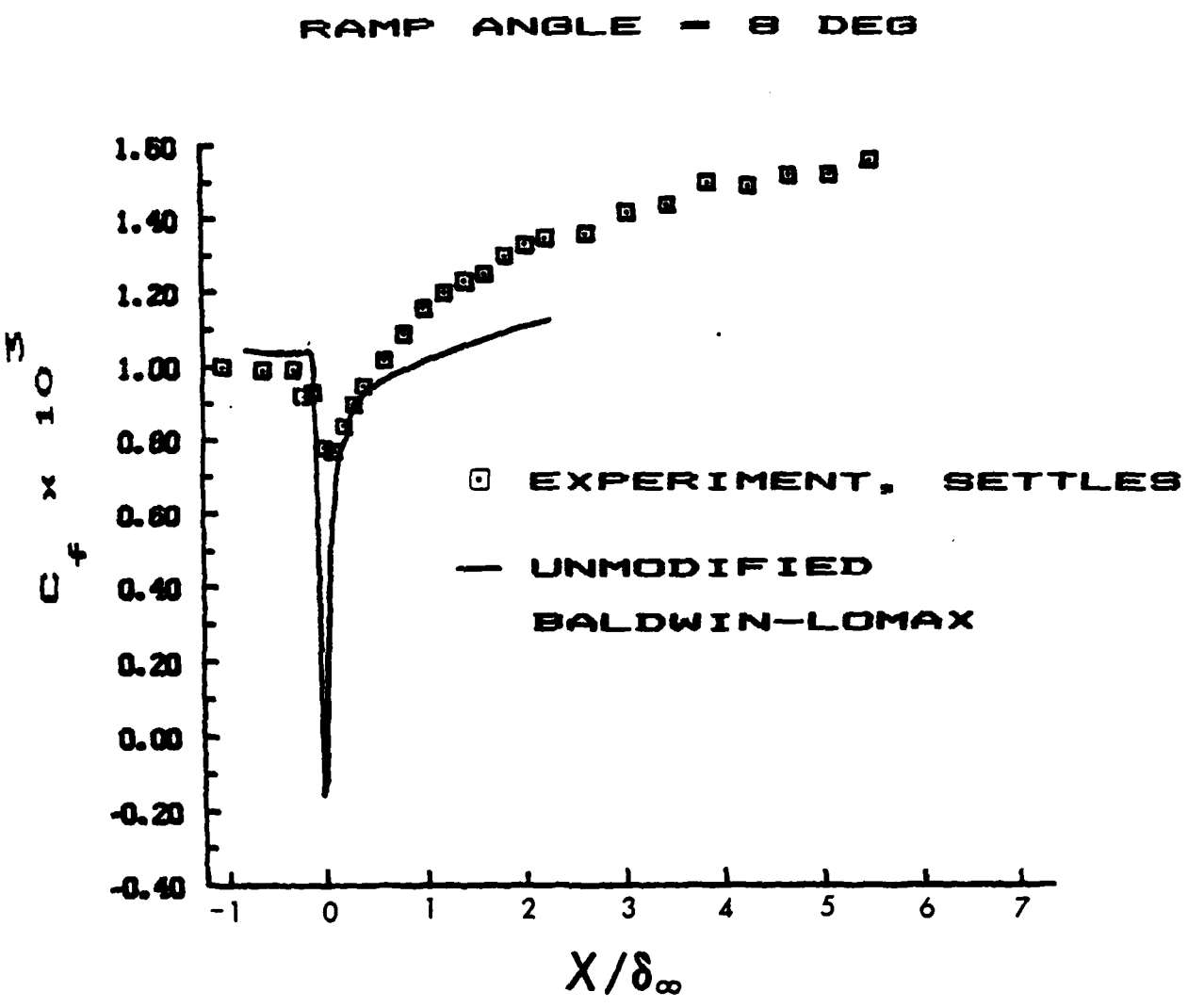

Fig. 3. Skin Friction Coefficient for $\alpha = 8°$

unmodified and modified Baldwin-Lomax model. The computed and measured surface pressure is shown in Fig. 4. The surface pressure results using the unmodified Baldwin-Lomax model are essentially identical to the modified model and are not shown. The computed profile displays an insufficient upstream propagation, similar to the results obtained by Shang and Hankey[14] using the unmodified Cebeci-Smith algebraic eddy viscosity model. The computed and measured profiles are seen to be in good agreement in the recovery region.

The computed and measured skin friction coefficient is displayed in Fig. 5. Results are shown for the two separate calculations, employing the unmodified Baldwin-Lomax model and the modified Baldwin-Lomax model. The computed and measured profiles show reasonable agreement in the region of rapidly decreasing skin friction. The computed separation-to-reattachment length is seriously overpredicted by the unmodified Baldwin-Lomax model. The modified model shows a substantial improvement in this regard. In the recovery region (i.e., downstream of reattachment), the modified model again displays a marked improvement over the original Baldwin-Lomax model. Both models, however, seriously underpredict the magnitude of the skin friction in the recovery region. This behavior is similar to previous computations using algebraic eddy viscosity models.[17]

The computed and experimental velocity profiles at three stations (corresponding to positions upstream, at the corner, and downstream of the interaction) are shown in Fig. 6. The computed profile downstream of reattachment displays an insufficient recovery near the wall (i.e., the computed velocity is below the experimental data). This observation is consistent with the underprediction of the skin friction discussed above.

4.3 Results for 20 deg Ramp

The computed and experimental surface pressure are displayed in Fig. 7,

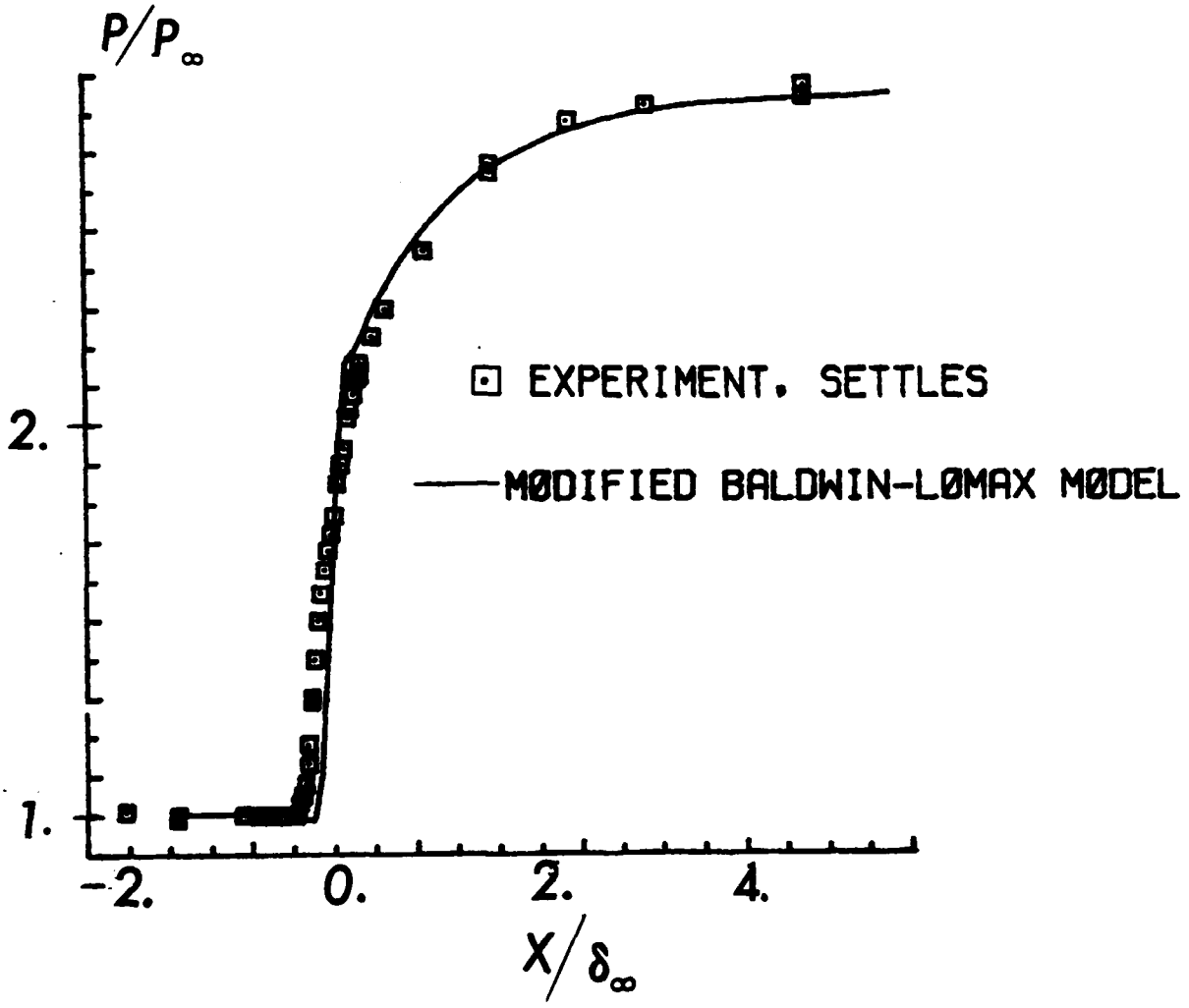

Fig. 4. Surface Pressure for α = 16 deg

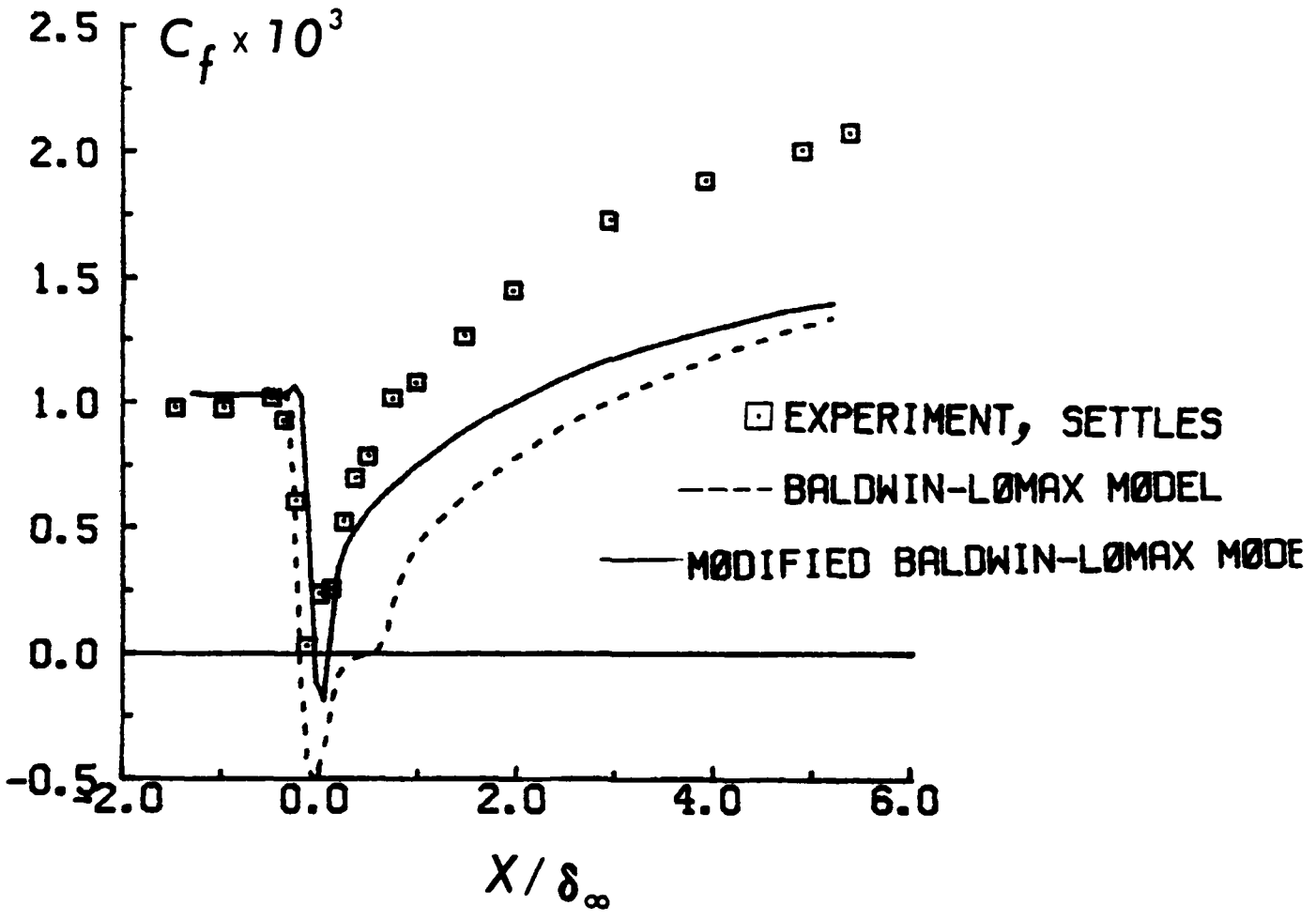

Fig. 5. Skin Friction Coefficient for α = 16 deg

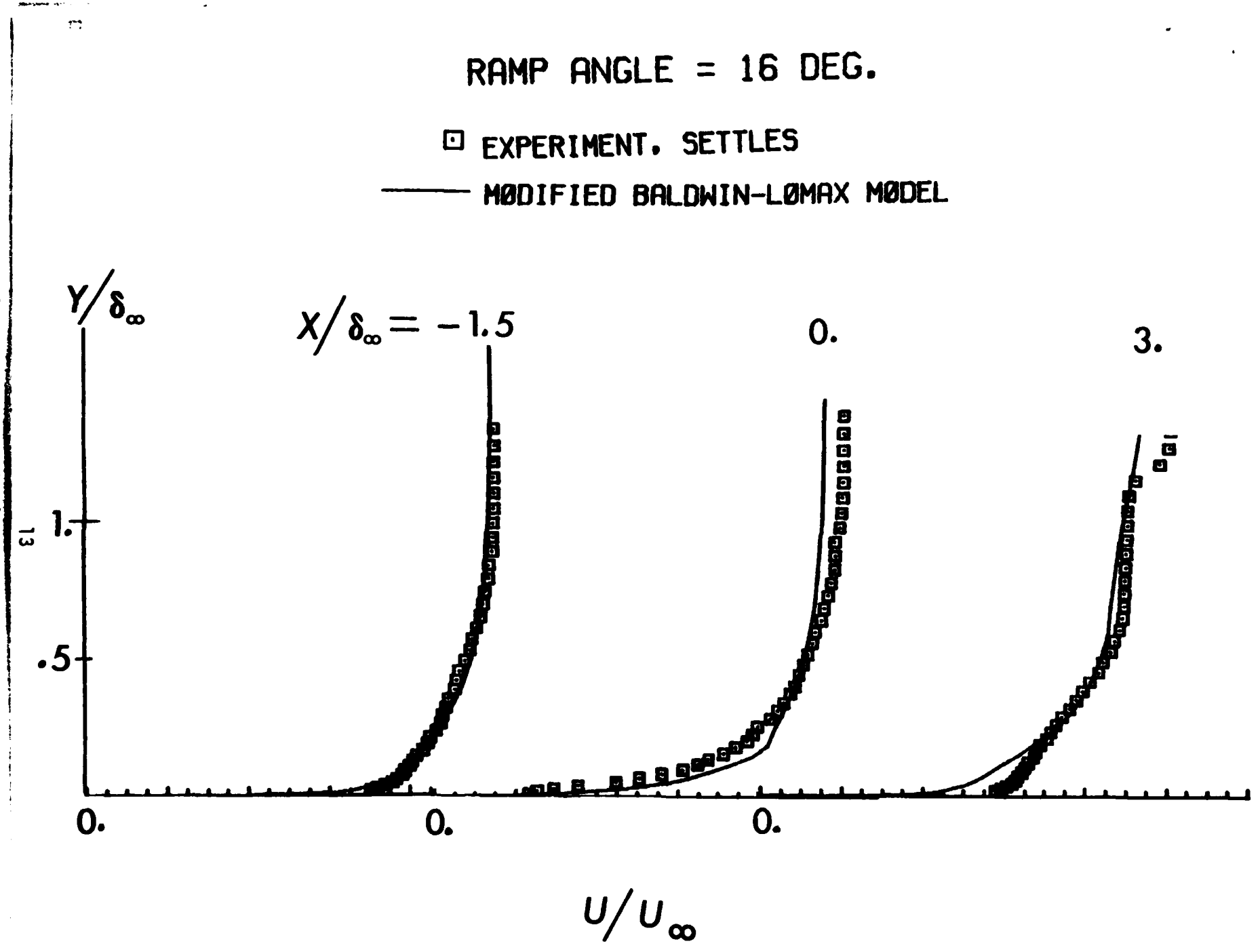

Fig. 6. Velocity Profiles for α = 16 deg

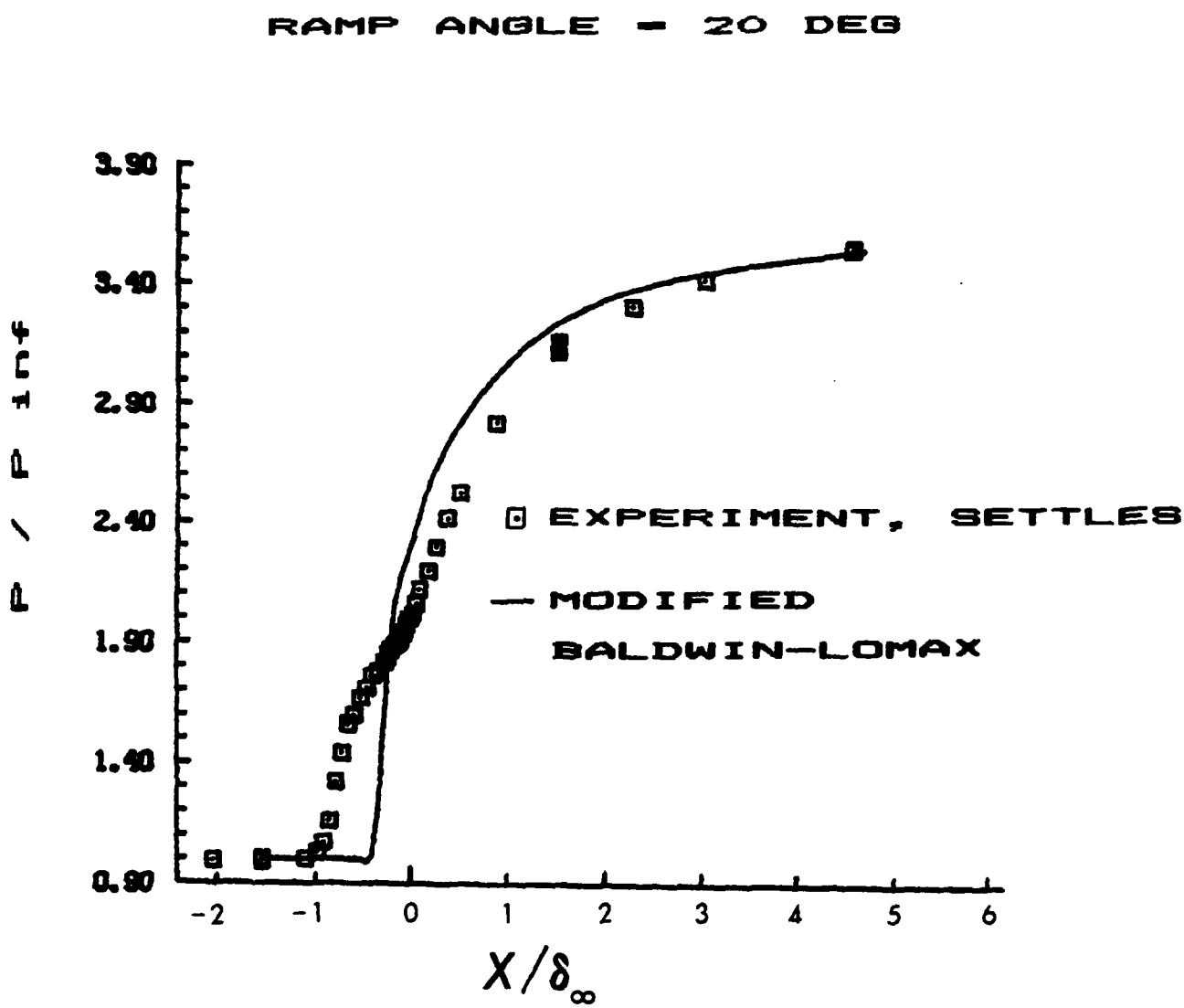

Fig. 7. Surface Pressure for α = 20 deg

where results are shown for the modified Baldwin-Lomax model. Due to the improvement afforded by the modified model, no further computations have been performed to date using the original unmodified model. The computed results again display an insufficient upstream propagation.

The skin friction is shown in Fig. 8. The computed skin friction begins to decrease at a location closer to the corner than the experimental data, due to the insufficient upstream propagation in the computed flowfield. The size of the separation region is overpredicted by the computations, and the recovery of the boundary layer is again less rapid than observed experimentally. Comparison of velocity profiles (not shown) affirms these conclusions.

4.4 Results for 24 deg Ramp

The computed and measured surface pressure for the 24 deg ramp are displayed in Fig. 9, which includes results for the modified and relaxation eddy viscosity models. The relaxation length was determined by requiring agreement between the computed and measured upstream propagation distance as determined by the surface pressure. It should be noted that the relaxation length of 10 δ_∞ employed by Shang and Hankey is substantially larger than required by the above criteria, and yields a significant overprediction of the extent of upstream propagation.

The computed and measured skin friction coefficient is shown in Fig. 10. Compared to the modified Baldwin-Lomax model, the relaxation model improves the prediction of the separation location. Both models, however, significantly underestimate the skin friction in the recovery region.

5. Conclusions to Date

Based upon the above results, the following conclusions have been made:

a. The unmodified Baldwin-Lomax model underestimates the upstream propagation of the interaction and the downstream recovery of

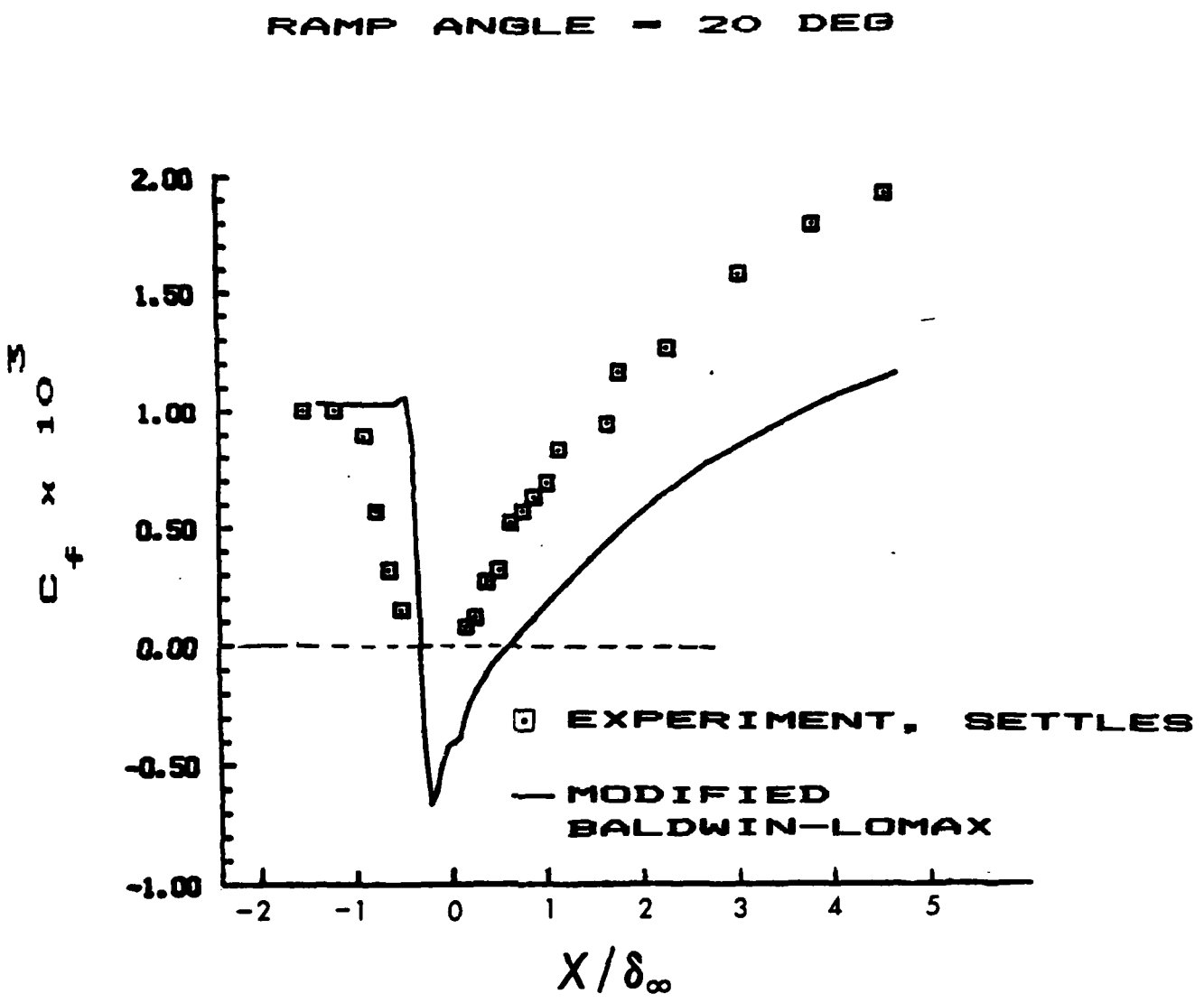

Fig. 8. Skin Friction Coefficient for α = 20 deg

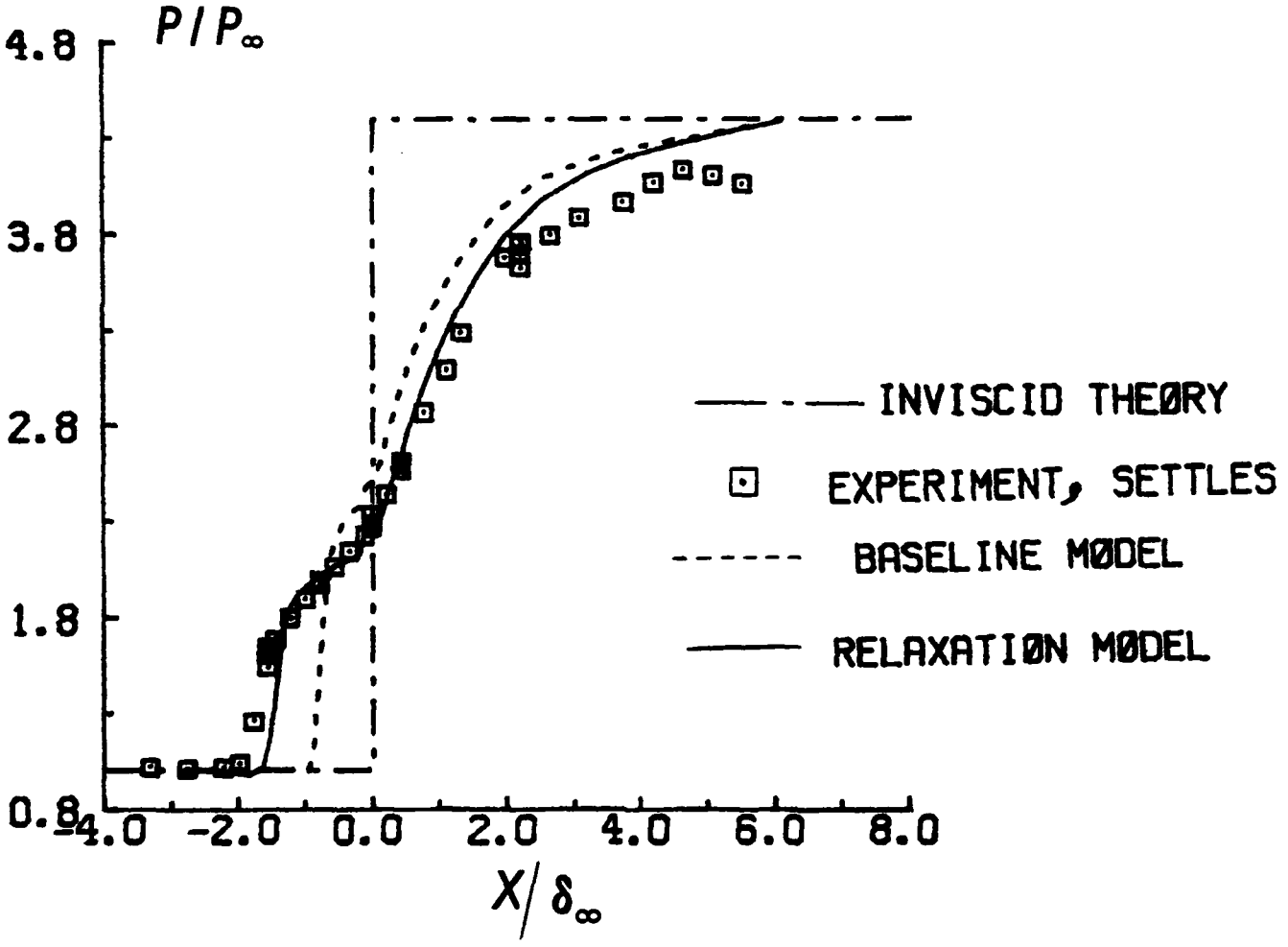

Fig. 9. Surface Pressure for α = 24 deg

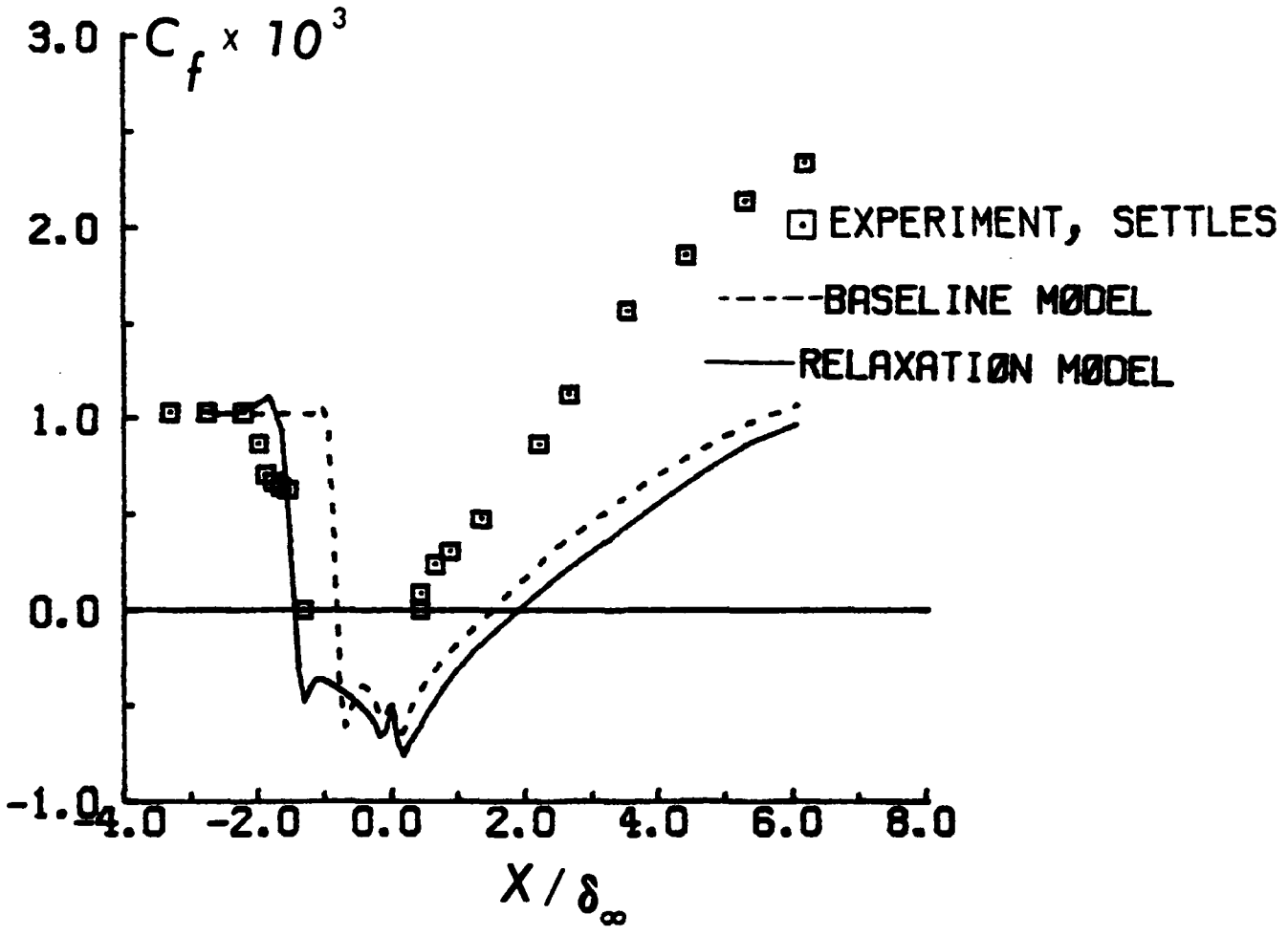

Fig. 10. Skin Friction Coefficient for α = 24 deg

the boundary layer.

b. The modified Baldwin-Lomax model provides some improvement in the location of reattachment at moderate ramp angles.

c. A relaxation length may be selected which provides good agreement with the upstream propagation of the interaction as seen in the surface pressure and skin friction profiles. The relaxation length is substantially smaller than employed by Shang and Hankey with the Cebeci-Smith turbulence model.

d. All versions of the turbulence model underpredict the recovery of the boundary layer downstream of reattachment.

e. The underprediction of the boundary layer recovery is attributable to the inability of the algebraic eddy viscosity model to incorporate the observed rapid increase in turbulent mixing downstream of reattachment.

6. Research Plans for Remainder of Second Year for Two-Dimensional Compression Ramp

During the remaining portion of the second year, additional studies of the 2-D compression ramp will be performed. First, several additional computations of the first category of experimental data at Mach 3 (variable ramp angle with fixed Re_{δ_∞}) will be performed with the modified and relaxation models. Secondly, the second category of experimental data at Mach 3 (variable Re_{δ_∞} and fixed ramp angle) will be considered. Thirdly, several additional computations of the 2-D compression ramp at Mach 2 are planned.

B. Calculation of Three-Dimensional Supersonic Sharp Fin Flows

1. Motivations

The purposes of the 3-D sharp fin investigations are twofold, namely

a. To critically examine the accuracy of theoretical predictions of a 3-D shock wave-turbulent boundary layer interaction using the Baldwin-Lomax model.

b. To evaluate the physical structure of the 3-D sharp fin interaction using the computed results.

As indicated in Section II.A.1, the Baldwin-Lomax model has been utilized for a variety of 3-D turbulent interaction calculations. The present investigation seeks to examine the accuracy of the Baldwin-Lomax model by comparison with the extensive experimental data base of Oskam and his colleagues.[18-21] It is recognized, of course, that the evaluation of the accuracy of the Baldwin-Lomax model is a necessary prerequisite to the utilization of the computed solution to examine the physical structure of the 3-D sharp fin flowfield.

2. Experimental Configuration

The flow configuration is illustrated in Fig. 11, and consists of a corner formed by a flat plate (i.e., wind tunnel wall) and a wedge ("shock generator"). An equilibrium supersonic turbulent boundary layer develops on a flat plate (i.e., wind tunnel wall). The deflection of the wedge surface results in the formation of an oblique shock, which intersects the turbulent boundary layer on the flat plate, resulting in a 3-D shock wave-turbulent boundary layer interaction. An extensive experimental data base has been acquired by Oskam and his colleagues[18-21] at the Princeton Gas Dynamics Laboratory at a nominal free-stream Mach number of 2.9. During the present investigation, two separate configurations were computed with nominal wedge angles α_g of 4 deg and 10 deg. The experimental data of Oskam includes (a) surface pressure, (b) heat transfer, (c) profiles of pitot pressure, static pressure, pitch and yaw angles, (e) total temperature profiles, and (f) oil flow visualization.

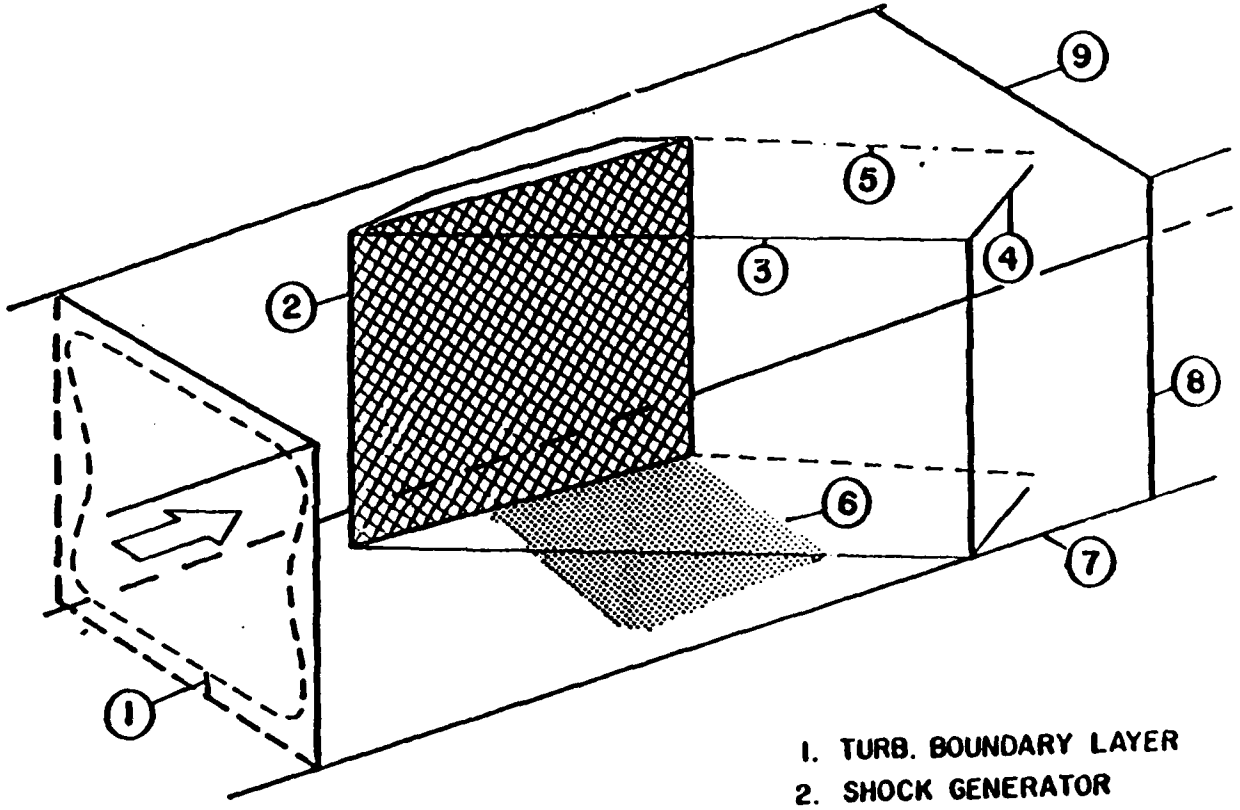

1. TURB. BOUNDARY LAYER
2. SHOCK GENERATOR
3. SHOCK WAVE FROM LEADING EDGE
4. SHOCK REFLECTED FROM SIDEWALL
5. EXPANSION FROM TRAILING EDGE
6. REGION OF STUDY
7. WINDTUNNEL BOTTOMWALL
8. WINDTUNNEL SIDEWALL
9. TOPWALL

Fig. 11. Geometry of 3-D Sharp Fin

3. Method of Solution

The governing equations are the full mean compressible Navier-Stokes equations in three dimensions using mass-averaged variables,[12] strong conservation form,[13] and general curvilinear coordinates. A perfect gas is assumed, and Sutherland's law is employed for the molecular viscosity. The molecular and turbulent Prandtl numbers are 0.72 (air) and 0.9, respectively.

The algebraic turbulent eddy viscosity model of Baldwin and Lomax is employed, with modification to the length scale for the corner region formed by the wedge and flat plate.[5,22,23] In addition, the outer formulation for the eddy viscosity was modified. Specifically, the function F_{max} was defined by the outermost extremum of the function $\ell\omega D$, where ℓ is the mixing length,[5,22,23] ω is the magnitude of the vorticity, and D is the Van Driest damping factor. This differs from the formulation proposed by Baldwin and Lomax, in which the maximum (not the outermost extremum within the boundary layer) defined F_{max} and ℓ_{max}. In the Van Driest damping factor, the wall value of the shear stress was employed. No relaxation model was utilized.

The numerical algorithm employed to solve the Navier-Stokes equations is the hybrid explicit-implicit algorithm developed by Knight.[24-27] The method combines the explicit finite-difference algorithm of MacCormack[28,29] with a separate implicit algorithm for the viscous sublayer and transition wall regions of the turbulent boundary layer. The algorithm has previously been employed for the computation of a variety of 2-D shock turbulent boundary layer interactions[24-26] (including cases in which flow separation occurred), and recently extended to 3-D flows. The overall algorithm is second-order accurate.

The incoming boundary layer profile, which provides the upstream boundary conditions for the computations, was obtained in the same manner as discussed previously. The computed upstream profile is in close agreement with the experiment and the compressible Law of the Wall and Wake.[16]

The general configuration of the computational domain is illustrated by the dotted lines in Fig. 12. The finite-difference grid consists of a number of streamwise planes, separated by a constant distance Δx. Within each streamwise plane, a highly non-uniform grid was employed to accurately resolve the boundary layer structure on the wedge and flat plate. The α_g = 3.73 deg case was computed using a total grid of 28,230 points, with a 38 by 29 grid distribution in the cross-plane. The α_g = 9.72 case was computed twice, using a total of 79,727 grid points (for Grid #1), and 34,232 points (for Grid #2). These two grid systems differed principally in the size of the streamwise grid spacing Δx, in order to evaluate the effect of the streamwise grid spacing on the computed solution. For Grid #1, $\Delta x = 0.46\ \delta_\infty$, and for Grid #2, $\Delta x = 0.93\ \delta_\infty$. The coarser grid spacing of Grid #2 is equal to that employed by Horstman and Hung.[30] Careful attention was devoted to insuring sufficient resolution of the flowfield by the grid, including the viscous sublayer and turbulent boundary layers. In particular, the distance of the first row of mesh points adjacent to the walls, expressed in wall units, was everywhere less than 3.2. Also, the typical number of points within the boundary layers on the flat plate and wedge are 20 and 17, respectively.

4. Results

Detailed comparison has been performed with the experimental data of Oskam for the nominal wedge angles of 4 deg and 10 deg for the Model 1 configuration of Oskam. Separate comparison has been performed for all of the published profiles of surface pressure, surface heat transfer, pitot pressure profiles, yaw angle profiles, static pressure profiles, and pitch angle profiles as given in Ref. 21. The streamwise location of the experimental measurement stations is displayed in Fig. 13. In the interest of brevity, results are presented herein

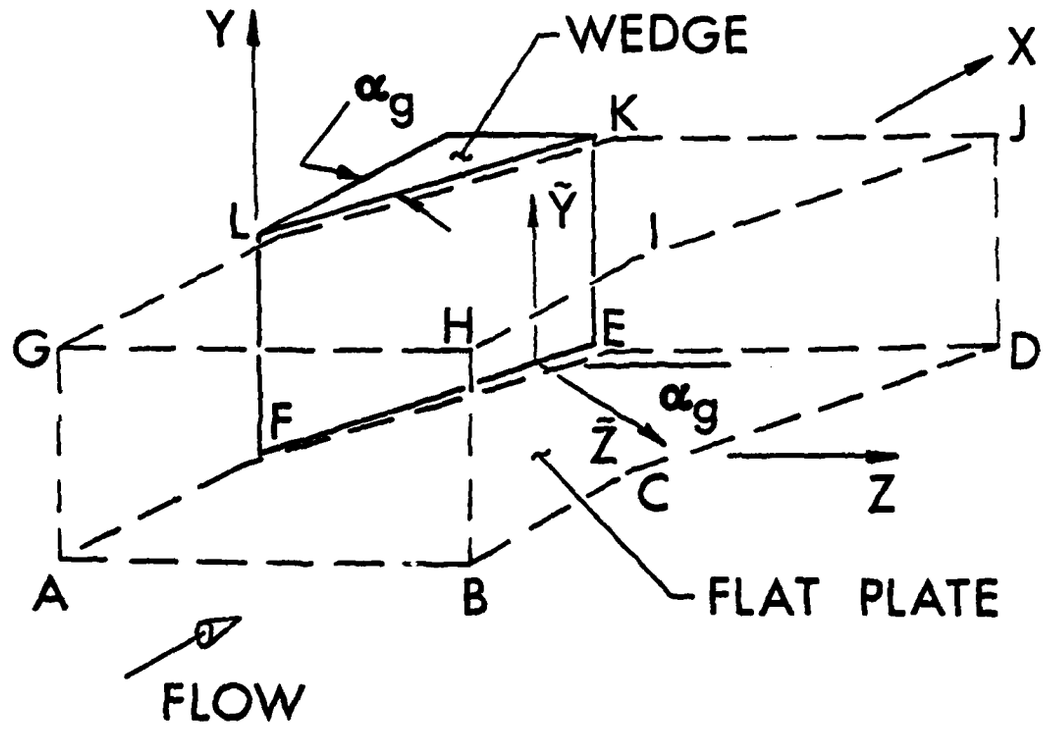

Fig. 12. Geometry of Computational Domain for 3-D Sharp Fin

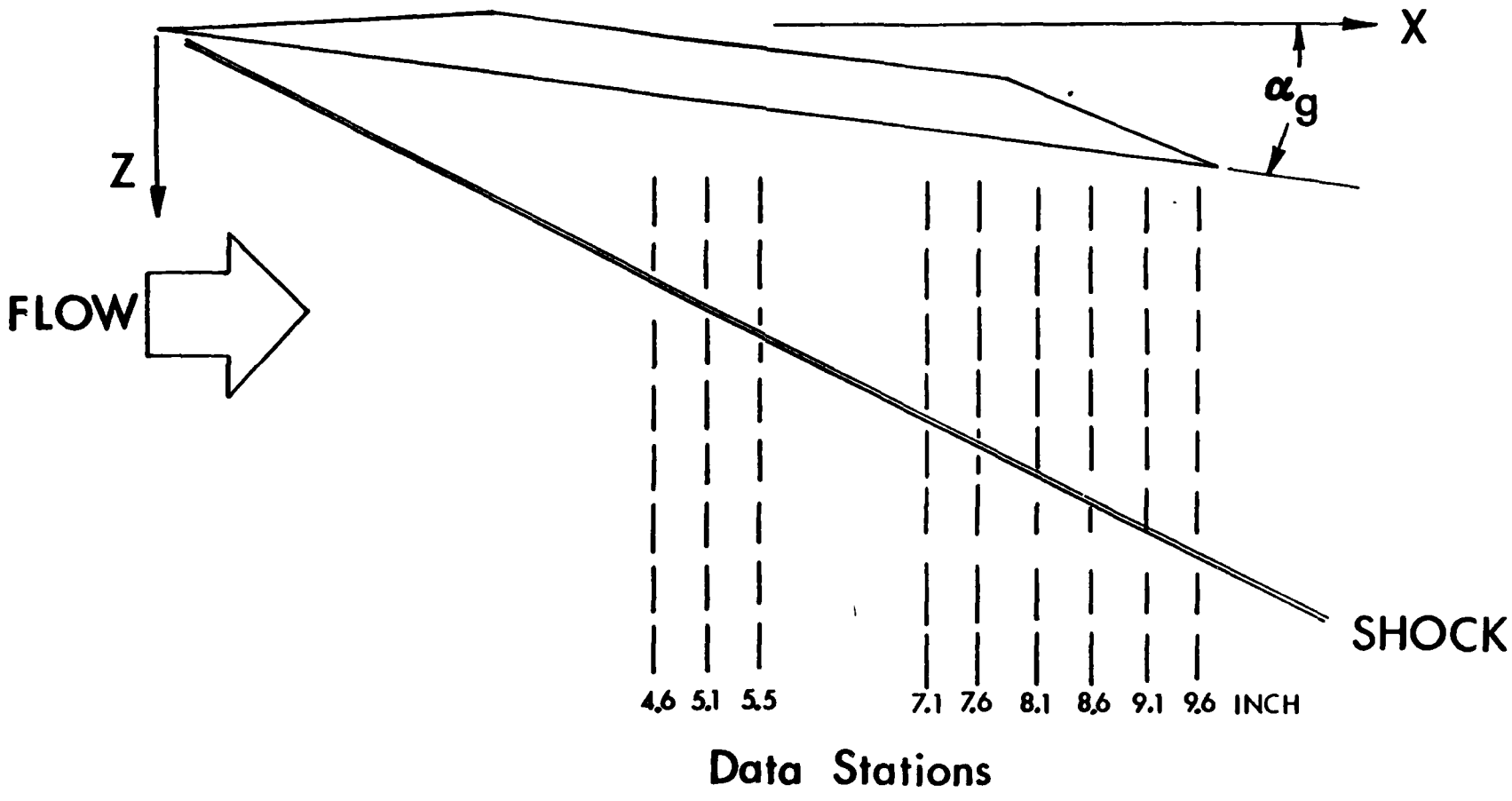

Fig. 13. Location of Experimental Data Stations

only for the α_g = 10 deg case at x = 14.1 δ_∞ (x = 7.6 inch = 19.3 cm).

The computed and experimental surface pressure on the flat plate at x = 14.1 δ_∞ is shown in Fig. 14. The arrow indicates the spanwise location of the shock wave at this station. The calculated profiles for Grid #1 (Δx = 0.46 δ_∞) and Grid #2 (Δx = 0.93 δ_∞) are seen to be in excellent agreement, with a maximum difference of 1%. The computed and measured pressure are in close agreement, with a maximum difference of less than 5%. The corner pressure agrees to within 3.6%. Additional comparison of profiles at x/δ_∞ = 8.46, 9.4, 10.4, 13.1, 14.9, 15.9 and 16.8 (not shown) indicates similar agreement. First, the maximum difference in computed profiles for Grid #1 and 2 is 1%. Second, the maximum difference between the calculated and experimental profiles at these stations is 3.3%, 5.4%, 4.0%, 5.0%, 6.0%, 7.0% and 4.0%, respectively. Third, the maximum overall difference between computed and experimental corner pressure is 4.0%. The computed profile of Horstman and Hung[30] at x = 14.1 δ_∞ shows similar close agreement with experiment.

In Fig. 15, the computed and experimental heat transfer coefficient on the flat plate at x = 14.1 δ_∞ is shown. The heat transfer coefficient is defined according to $C_h = q_w/\rho_\infty U_\infty c_p (T_w - T_{a_w})$ where q_w is the wall heat transfer, T_w is the wall temperature, and T_{a_w} is the adiabatic wall temperature. For the computed results, $T_{a_w} = T_\infty + r(T_{t_\infty} - T_\infty)$ where r = 0.89 is the recovery factor, which conforms with Oskam.[21] In normalizing with respect to C_{h_∞}, the corresponding experimental and calculated values of C_{h_∞} (0.00071 and 0.000656, respectively) are used. Although these values differ by 8.2%, this discrepancy is within the uncertainty of the experimental measurements[21] (±15% of C_{h_∞}). The computed profiles for Grids #1 and 2 are in good agreement, except for the pronounced "kink" in C_h for Grid #1 at z_g/δ_∞ = 0.2. This kink is associated with the Baldwin-Lomax turbulence model, and a complete discussion is presented

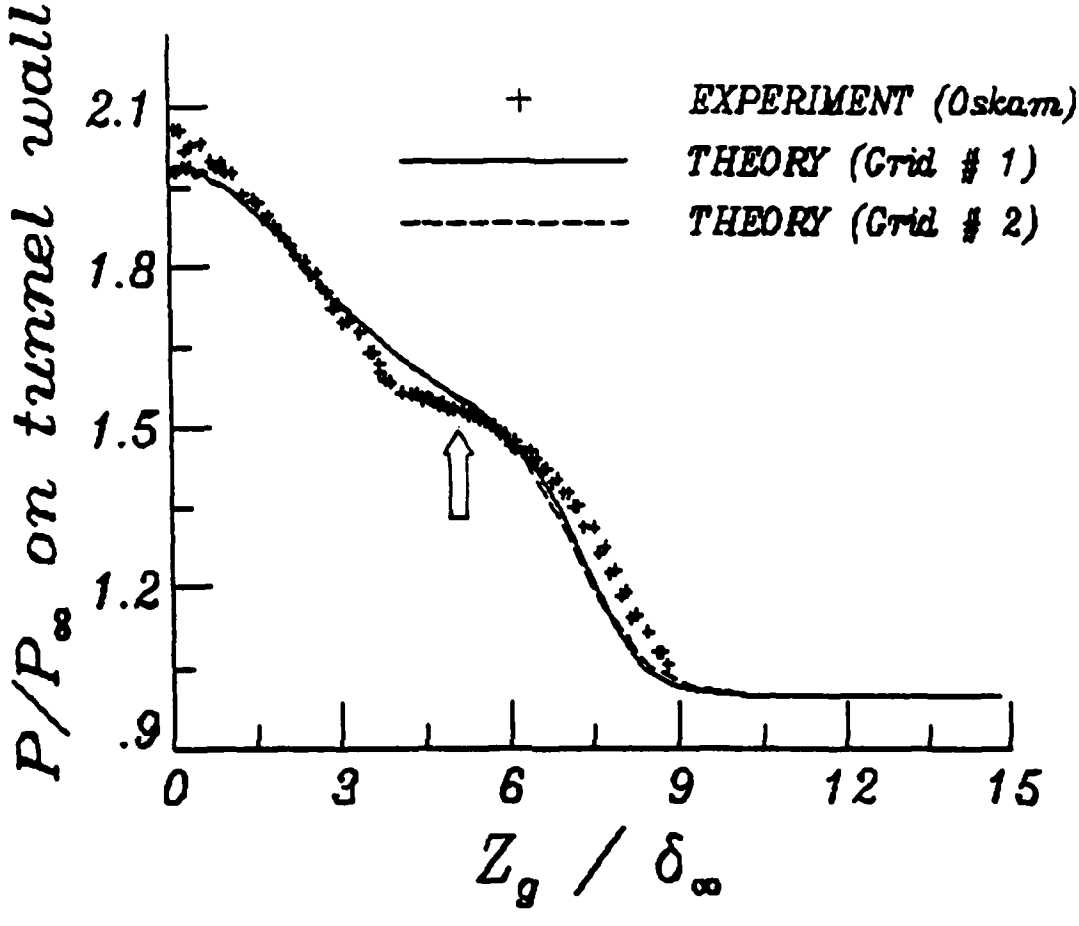

Fig. 14. Surface Pressure on Tunnel Wall at $x = 14.1\ \delta_\infty$ for $\alpha_g = 10$ deg

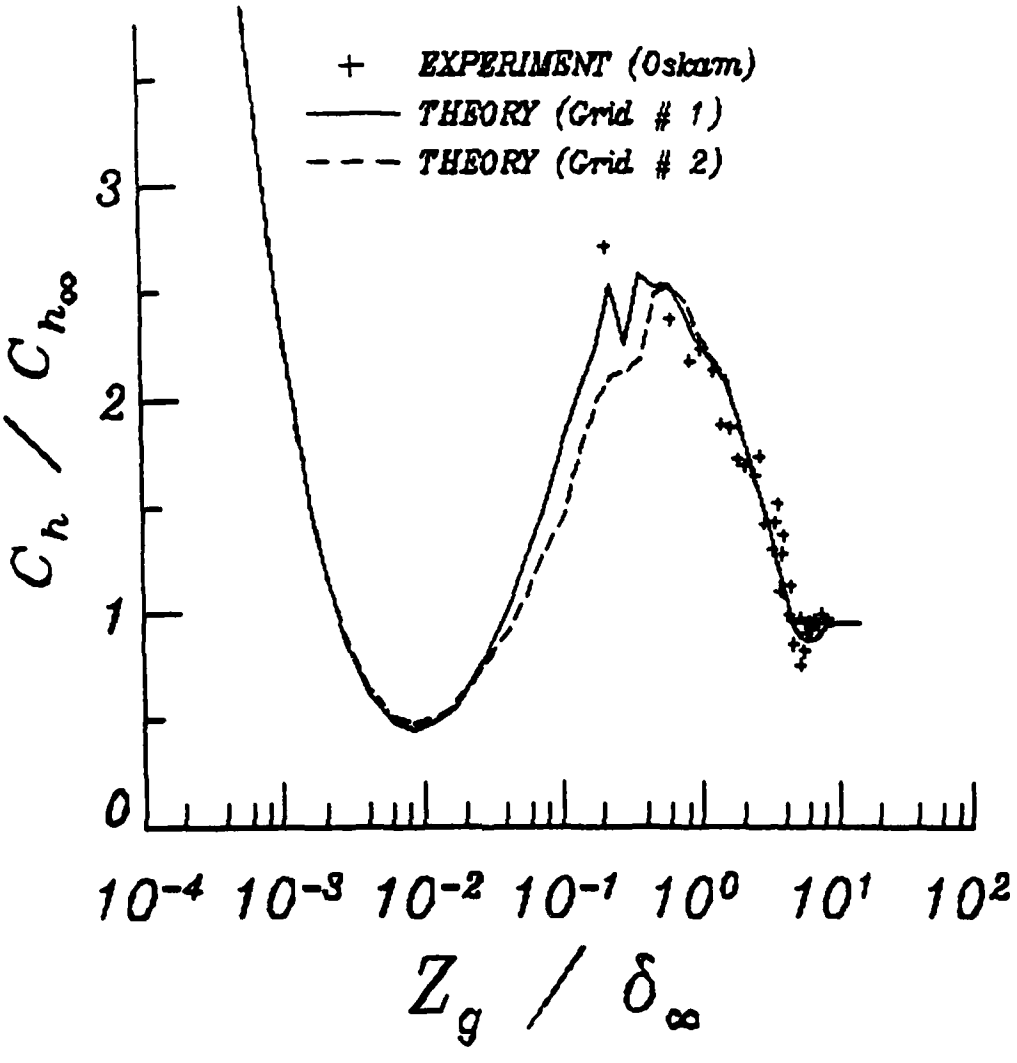

Fig. 15. Surface Heat Transfer on Tunnel Wall at $x = 14.1\ \delta_\infty$ for $\alpha_g = 10$ deg

in Ref. 27. The computed peak heat transfer coefficient is 7.2% below the experimental value, which is within the uncertainty of the measurement. Comparison with three additional profiles at x/δ_∞ = 8.5, 9.4 and 13.1 display similar agreement. First, the difference in computed peak heat transfer between Grid #1 and 2 is less than 5.5% at all stations. Second, the difference in the computed peak C_h (using Grid #1) and experiment is 3.8%, 5.5% and 8.0%, respectively, at the three stations.

The computed and measured yaw angle at two spanwise locations (z_g/δ_∞ = 0.47 and 4.2) at x = 14.1 δ_∞ is shown in Fig. 16. The yaw angle is defined by $\alpha = \tan^{-1}(w/u)$ where u and w are the components of the velocity along the x and z directions (Fig. 12). At this x-station, the shock is located at z_g/δ_∞ = 5.03. The computed profiles using Grid #1 and 2 are seen to be in excellent agreement, with only a slight difference in the inviscid region at z_g/δ_∞ = 4.2 which is less than 2 deg. The calculated profile at z_g/δ_∞ = 0.47 is in excellent agreement with the experiment. The comparison at z_g/δ_∞ = 4.2 displays good agreement, with a maximum difference of 4.8 deg. The rapid increase of yaw angle within the boundary layer is evident, with values reaching 36 deg close to the flat plate. Comparison with 18 additional profiles (not shown) confirm the above findings. First, the computed profiles using Gird #1 and 2 are in excellent agreement. The maximum difference within the boundary layer is less than 1 deg, and the maximum difference outside the boundary layer is less than 2 deg. Second, the computed profiles are in good agreement with the experiment. Specifically, comparison of profiles for $z_g/z_{g_{s(x)}}$ between 0 and 0.7 (where $z_{g_{s(x)}}$ is the shock location) indicate a maximum difference of less than 3 deg. For $z_g/z_{g_{s(x)}}$ between 0.7 and 1.45 (the spanwise limit of the measurements), the maximum difference is less than 6 deg.

In Fig. 17, two profiles of the calculated and experimental pitot pressure p_p at $x = 14.1\ \delta_\infty$ are shown. The spanwise locations are the same as for Fig. 16. The computed profiles using Grid #1 and 2 are in close agreement within the boundary layer, with a maximum difference of 4.7% at $z_g/\delta_\infty = 0.47$ and less than 1% at $z_g/\delta_\infty = 4.2$. The computed profiles display a maximum difference of 6.8% in the inviscid region at $z_g/\delta_\infty = 4.2$, which is associated with the proximity of this location to the shock and the shock-capturing nature of the algorithm. The calculated profiles are observed to be in good agreement with the experiment. At $z_g/\delta_\infty = 0.47$, the maximum difference between the calculated and measured profiles is less than 5% everywhere (except for the data point nearest the plate, which is at $y = 0.0254$ cm). At $z_g/\delta_\infty = 4.2$, the maximum difference is less than 9.0% of p_{p_∞}. Comparison with 18 additional profiles (not shown) shows similar characteristics. First, the computed profiles using Grids #1 and 2 are in excellent agreement. The maximum difference within the boundary layer is less than 1%, except for three profiles (at different x) close to the corner (z_g/δ_∞ typically equal to 0.1) for which the maximum difference is less than 5%. Second, the computed profiles are in reasonable agreement with experiment. The maximum difference between the computed and experimental results is less than 10% for 15 of the 18 profiles, and less than 15.6% for the remaining profiles.

In Fig. 18, the direction and magnitude of the surface shear stress on the flat plate is shown (only even-numbered x-stations have been plotted for clarity using the solution from Grid #1). The experimental oil film pattern is shown in Fig. 19. The flow geometry in Fig. 18 has been reflected in the x-y plane in order to agree with the flowfield orientation of Fig. 19. It is apparent from Fig. 19 that a line of coalescence (denoted a "three-dimensional separation line;"[31] see also Ref. 32) forms upstream of the shock location. The computed coalescence line, which also represents an asymptote of the surface shear stress, is in

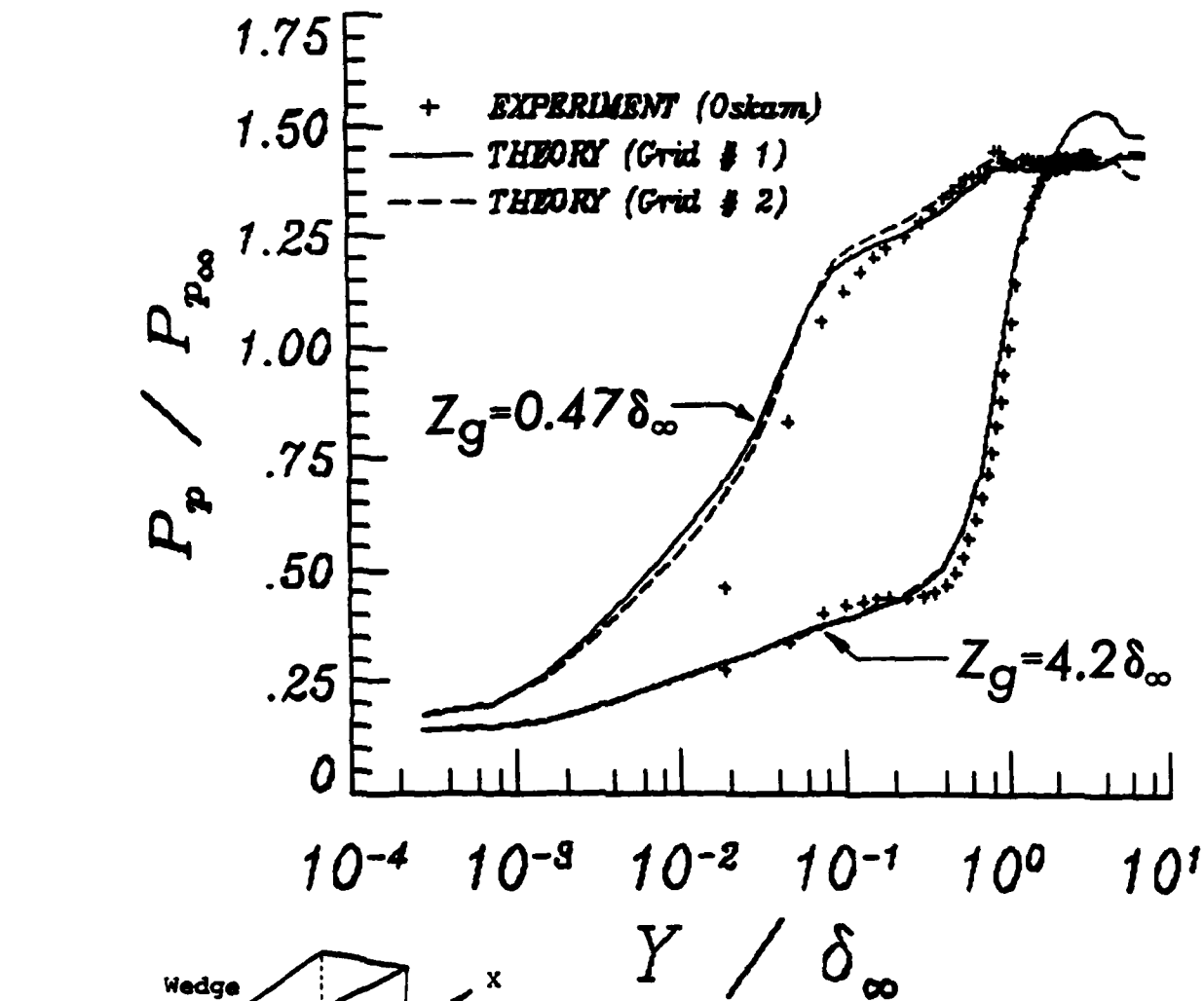

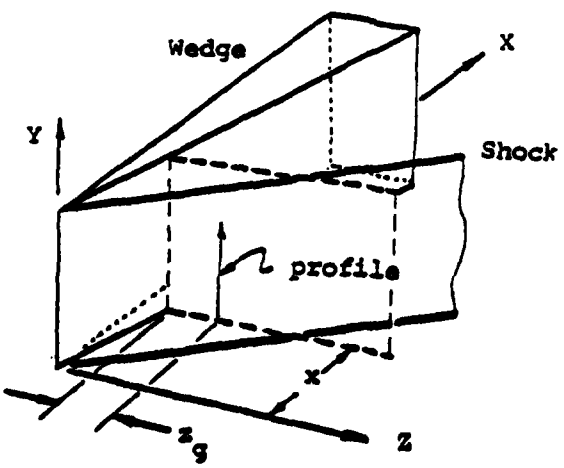

Fig. 17. Pitot Pressure at x = 14.1 δ_∞ for α_g = 10 deg

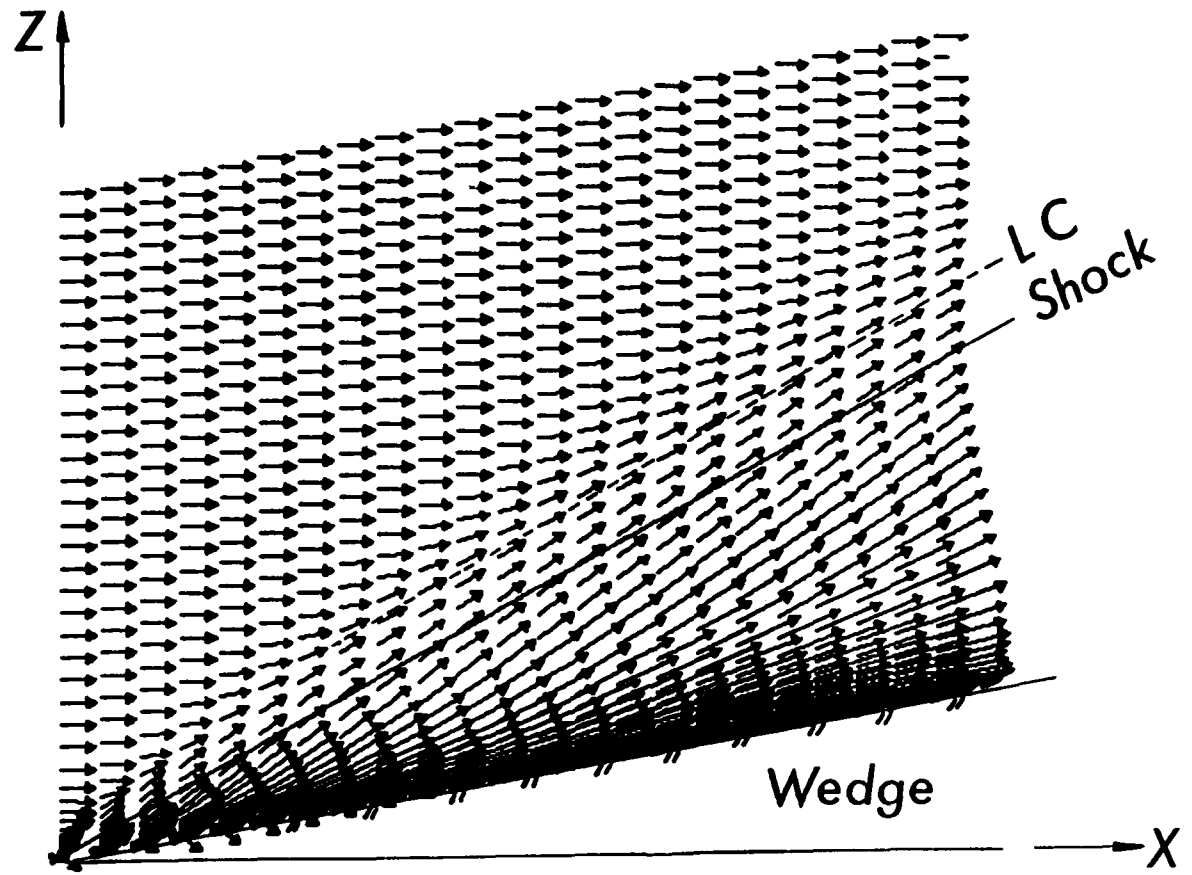

Fig. 18. Computer Shear Stress on Tunnel Wall for α_g = 10 deg (Wedge has been moved to right side for ease of comparison with Fig. 19)

Fig. 19. Experimental Oil Flow Pattern on Tunnel Wall for α_g = 10 deg

good agreement with the experimental oil film coalescence line. In particular, at x/δ_∞ = 10.0, the normal distance of the coalescence line from the shock line is approximately 1.2 δ_∞ in the experiment and 1.3 δ_∞ in the calculation. Computations by Horstman and Hunt[30] of the flow streamlines for this and other cases exhibiting coalescence of the surface shear stress have shown a strong lifting off of the fluid in the vicinity of the line of coalescence. Additional investigation of the flowfield in this region is needed.

5. Conclusions to Date

Based upon the extensive comparison between computed results and the experimental data of Oskam,[21] it is concluded that the theoretical results using the Baldwin-Lomax turbulence model provide good agreement with the experimental data for the configurations examined for a wide variety of flow variables including surface pressure, heat transfer, pitot pressure, static pressure and yaw angle. This comparison, therefore, provides the necessary confidence in the accuracy of the Baldwin-Lomax model for the configurations examined, and thus permits the use of the computed flowfields for α_g = 3.73 deg and 9.72 deg for the examination of additional details of the flowfield structure.

6. Research Plans for Remainder of Second Year for 3-D Turbulent Interactions

The research schedule for the remaining portion of the second year may be categorized into two major areas:

a. Investigation of Flowfield Structure for the 3-D Sharp Fin (α_g = 3.73 deg and 9.72 deg).

The physical structure of the 3-D sharp fin flowfield will be examined using the computed results. A variety of possible areas may be considered, including examination of cross-flow velocity

vectors (in order to investigate possible "vortical" flow structures) and streamline and streamtube tracing (to examine the fluid particle motion, particularly in the vicinity of the line of coalescence).

b. Computation of 3-D Swept Compression Corner at Mach 3.

One or more configurations of the swept compression corner will be computed, and the results compared with the experimental data of Settles et al.[2,33] This investigation will provide further examination of the efficacy of the Baldwin-Lomax turbulence model, and, assuming good agreement between the computed and experimental data, the opportunity for further investigation of the flowfield structure using the computed results.

III. Written Publications

1. Visbal, M., and Knight, D., "Generation of Orthogonal and Nearly Orthogonal Coordinates with Grid Control Near Boundaries," AIAA J., Vol. 20, No. 3, March 1982, pp. 305-306.
2. Knight, D., "Application of Curvilinear Coordinate Generation Techniques to the Computation of Internal Flows," in Numerical Grid Generation - Proceedings of a Symposium on the Numerical Generation of Curvilinear Coordinates and their Use in the Numerical Solution of Partial Differential Equations, North-Holland, New York, 1982, pp. 357-384.
3. Knight, D., "A Hybrid Explicit-Implicit Numerical Algorithm for the Three-Dimensional Compressible Navier-Stokes Equations," AIAA Paper No. 83-0223, AIAA 21st Aerospace Sciences Meeting, January 10-13, 1983.

Publication No. 1 represents research sponsored by AFOSR Grant 80-0072 and AF Contract F-33615-C-3008.

Publications No. 2 and 3 represent research sponsored by AFOSR Grants 80-0072 and 82-0040.

IV. List of Personnel

Principal Investigator: Prof. Doyle Knight
Department of Mechanical and Aerospace Engineering

Graduate Research Assistant: Mr. Miguel Visbal
Department of Mechanical and Aerospace Engineering

V. Interactions

A. Interactions with Research Group at Princeton Gas Dynamics Laboratory

The interaction with the Princeton Gas Dynamics Laboratory can be categorized into three main areas:

a. Frequent Meetings with Princeton Research Personnel Throughout the Year

Frequent meetings have been held with the research personnel at Princeton. The purpose of these meetings has been to discuss the results of the theoretical research, and to propose future directions for the research effort. These meetings have proven very fruitful.

b. Computation of Flowfields Previously Investigated at Princeton

The 2-D compression ramp and 3-D sharp fin experimental data were obtained at Princeton during the mid-1970s. The choice of these data bases has allowed a close interaction with the Princeton group in the discussion of the computed results. All comparisons between computed and experimental results have been provided to the Princeton research group.

c. Comparison of Computed Pitot Pressure and Yaw Angle Profiles with the Experimental Surveys for the 3-D Sharp Fin at Mach 3 Taken at Princeton During 1982

A set of twenty-two profiles each of pitot pressure and yaw angle for the 3-D sharp fin at α_g = 9.72 deg was compared with the experimental data obtained at Princeton during 1982. These profiles examined

additional features of the flowfield which had not been investigated by Oskam.[18-21] The entire set of profile comparisons was provided to the Princeton group, and the results discussed at a meeting in October '82. The experimental data showed a distinct "bulge" in the yaw angle immediately above the tunnel wall boundary layer and slightly upstream of the shock wave. This "bulge" was also evident in the calculated results, although quantitatively not as large. Precise comparison between computed and measured results in this case was feasible for most (although not all) of the experimental profiles. In particular, comparison was mitigated by the close proximity of several of the experimental data stations to the shock location (i.e., within 0.5 δ_∞) and the shock-capturing nature of the numerical algorithm. It is also noted that the experimental data profiles were transferred by asynchronous transmission between the computer at the Princeton Gas Dynamics Lab and a computer at Rutgers University with the assistance of Mr. Dick Gilbert of Princeton.

B. Spoken Papers Presented at Technical Meetings for the Period 1 Oct 1981 to 30 Sept 1982

1. Knight, D., "Computation of Three-Dimensional Viscous-Inviscid Interactions on the CYBER 203 Vector-Processing Computer," Thirty-Fourth Meeting of the American Physical Society, Division of Fluid Dynamics, November 1981; Bulletin of the American Physical Society, Vol. 26, November 1981, p. 1248.

C. Seminars for the Period 1 Oct 1981 to 30 Sept 1982

1. Knight, D., "Computation of Three-Dimensional Compressible Viscous Flows on the CYBER 203 Computer," Courant Institute of Mathematical Sciences, New York, January 1982.

2. Knight, D., "Numerical Simulation of High Speed Viscous Flows," Dept. of Aerospace Engineering, Texas A&M University, April 1982.

3. Knight, D., "Generation of Water Waves by Wind," Dept. of Meteorology, Cook College, Rutgers University, April 1982.

D. Invited Lectures for the Period 1 Oct 1981 to 30 Sept 1982

1. Knight, D., "Application of Curvilinear Coordinate Generation Techniques to the Computation of Internal Flows," Symposium on Numerical Generation of Curvilinear Coordinates and their Use in the Numerical Solution of Partial Differential Equations, Nashville, Tennessee, April 1982 (see Section III).

VI. References

1. Korkegi, R., "Survey of Viscous Interactions Associated with High Mach Number Flight," AIAA J., Vol. 9, 1971, pp. 771-784.
2. Settles, G., Perkins, J., and Bogdonoff, S., "Investigation of Three-Dimensional Shock/Boundary-Layer Interactions at Swept Compression Corners," AIAA J. Vol. 18, 1980, pp. 779-785.
3. Knight, D., "Theoretical Investigation of Three-Dimensional Shock Wave-Turbulent Boundary Layer Interactions," Proposal Submitted to Air Force Office of Scientific Research, June 1981.
4. Baldwin, B., and Lomax, H., "Thin Layer Approximation and Algebraic Model for Separated Turbulent Flow," AIAA Paper 78-257, 1978.
5. Hung, C., and MacCormack, R., "Numerical Solution of Three-Dimensional Shock Wave and Turbulent Boundary Layer Interaction," AIAA Paper 78-161, 1978.
6. Deiwert, G, "Numerical Simulation of Three-Dimensional Boattail Afterbody Flowfields," AIAA J., Vol. 19, 1981, pp. 582-588.
7. Hung, C., and Chaussee, D., "Computation of Supersonic Turbulent Flows Over an Inclined Ogive-Cylinder Flare," AIAA Paper 80-1410, 1980.
8. Shang, J., "Numerical Simulation of Wing-Fuselage Interference," AIAA Paper 81-0048, 1981.
9. Settles, G., Bogdonoff, S., and Vas, I., "Incipient Separation of a Supersonic Turbulent Boundary Layer at High Reynolds Number," AIAA J., Vol. 14, 1976, pp. 50-56.
10. Settles, G., Fitzpatrick, T., and Bogdonoff, S., "Detailed Study of Attached and Separated Compression Corner Flowfields in High Reynolds Number Supersonic Flow," AIAA J., Vol. 17, 1979, pp. 579-585.
11. Settles, G., Gilbert, R., and Bogdonoff, S., "Data Compilation for Shock Wave/Turbulent Boundary Layer Interaction Experiments on Two-Dimensional

Compression Corners," Report MAE-1489, Dept. of Mech. and Aero. Engr., Princeton U., 1980.

12. Rubesin, M., and Rose, W., "The Turbulent Mean-Flow, Reynolds-stress, and Heat-flux Equations in Mass-Averaged Dependent Variables," NASA TMX-62248, March 1973.

13. Pulliam, T., and Steger, J., "Implicit Finite-Difference Simulations of 3-D Compressible Flows," AIAA J., Vol. 18, 1980, pp. 159-167.

14. Shang, J., and Hankey, W., "Numerical Solution for Supersonic Turbulent Flow Over a Compression Ramp," AIAA J., Vol. 13, 1975, pp. 1368-1374.

15. Beam, R., and Warming, R., "An Implicit Factored Scheme for the Compressible Navier-Stokes Equations," AIAA J., Vol. 16, 1978, pp. 393-402.

16. Sun, C.-C., and Childs, M. "Wall-Wake Velocity Profile for Compressible Nonadiabatic Flows," AIAA J., Vol. 14, 1976, pp. 820-822.

17. Horstman, C., Hung, C., Settles, G., Vas, I., and Bogdonoff, S., "Reynolds Number Effects on Shock-Wave Turbulent Boundary Layer Interaction - A Comparison of Numerical and Experimental Results," AIAA Paper 77-42, 1977.

18. Oskam, B., Vas, I., and Bogdonoff, S., "Mach 3 Oblique Shock Wave/Turbulent Boundary Layer Interactions in Three Dimensions," AIAA Paper 76-336, 1976.

19. Oskam, B., Vas, I., and Bogdonoff, S., "An Experimental Study of Three-Dimensional Flow Fields in an Axial Corner at Mach 3," AIAA Paper 77-689, 1977.

20. Oskam, B., "Three-Dimensional Flow Fields Generated by the Interaction of a Swept Shock Wave with a Turbulent Boundary Layer," Princeton Gas Dynamics Lab, Report No. 1313, Dec. 1976.

21. Oskam, B., Vas, I., and Bogdonoff, S., "Oblique Shock Wave/Turbulent Boundary Layer Interactions at Mach 3," AFFDL-TR-76-48, Part I (1976), Part II (1978), Air Force Flight Dynamics Laboratory, Wright-Patterson AFB, Ohio.

22. Shang, J., Hankey, W., and Petty, J., "Three-Dimensional Supersonic Interacting Turbulent Flow Along a Corner," AIAA J., Vol. 17, 1979, pp. 706-713.

23. Gessner, F., and Po, J., "A Reynolds Stress Model for Turbulent Corner Flows - Part II: Comparison Between Theory and Experiment," J. Fluids Engr., Trans. of ASME, Vol. 98, Series 1, No. 2, 1976, pp. 269-277.

24. Knight, D., "Improved Calculation of High Speed Inlet Flows. Part I: Numerical Algorithm," AIAA J., Vol. 19, 1981, pp. 34-41.

25. Knight, D., "Improved Calculation of High Speed Inlet Flows. Part II: Results," AIAA J., Vol. 19, 1981, pp. 172-179.

26. Knight, D., "Calculation of High Speed Inlet Flows Using the Navier-Stokes Equations," J. Aircraft, Vol. 18, 1981, pp. 748-754.

27. Knight, D., "A Hybrid Explicit-Implicit Numerical Algorithm for the Three-Dimensional Compressible Navier-Stokes Equations," AIAA Paper 83-0223, January 1983.

28. MacCormack, R., "Numerical Solution of the Interaction of a Shock Wave with a Laminar Boundary Layer," Lecture Notes in Physics, Vol. 8, 1971, pp. 151-163.

29. Baldwin, B., and MacCormack, R., "A Numerical Method for Solving the Navier-Stokes Equations with Application to Shock-Boundary Layer Interactions," AIAA Paper 75-1, 1975.

30. Horstman, C., and Hung, C., "Computation of Three-Dimensional Turbulent Separated Flows at Supersonic Speeds, AIAA Paper 79-0002, 1979.

31. Peake, D., "Three-Dimensional Swept Shock/Turbulent Boundary Layer Separations with Control by Air Injection," Aeronautic Report LR-592, National Research Council-Canada, July 1976.

32. Kubota, H., and Stollery, J., "An Experimental Study of the Interaction Between a Glancing Shock Wave and a Turbulent Boundary Layer," J. Fluid Mech., Vol. 116, pp. 431-458.

33. Settles, G., Perkins, J., and Bogdonoff, S., "Upstream Influence Scaling of 2-D and 3-D Shock/Turbulent Boundary Layer Interactions at Compression Corners," AIAA Paper 81-0334, 1981.

END

DATE
FILMED

5 -83

DTIC